Journal of Crystal Growth 88 (1988) 193–204
North-Holland, Amsterdam

THERMODYNAMIC ANALYSIS AND PHASE EQUILIBRIA CALCULATIONS FOR THE Zn–Te, Zn–Se AND Zn–S SYSTEMS

Romesh C. SHARMA

Department of Metallurgical Engineering, Indian Institute of Technology, Kanpur, UP 208016, India

and

Y. Austin CHANG

Department of Metallurgical and Mineral Engineering, University of Wisconsin, Madison, Wisconsin 53706, USA

Received 1 June 1987; manuscript received in final form 19 November 1987

The available thermodynamic and phase equilibria data for the binary systems Zn–Te, Zn–Se and Zn–S have been analyzed using an "associated solution model" for the liquid phases and considering the ZnTe, ZnSe and ZnS phases as line compounds. The phase diagrams and thermodynamic properties calculated from the optimized phase parameters agree well with the experimental data.

1. Introduction

The Zn–chalcogen systems (i.e. Zn–Te, Zn–Se and Zn–S) are of considerable technological interest due to the semiconducting properties of the compounds ZnTe, ZnSe and ZnS. A knowledge of the phase equilibria and thermodynamic properties of these systems is of importance for the growth of zinc chalcogenide crystals by liquid phase epitaxy (LPE) or by other means. Each of these three binary systems, Zn–Te, Zn–Se and Zn–S, is characterized by the formation of a single, essentially stoichiometric, intermediate compound, ZnX (X = Te, Se or S, respectively). These compounds normally (i.e. at atmospheric pressure) dissociate/sublime at higher temperatures; however, they do melt congruently under high pressures. The Zn–X phase diagrams as reported in the literature or discussed herein are therefore projections of the P–T–x diagrams onto the T–x plane, P, T and x being pressure, temperature and composition, respectively. However, the effect of pressure on the condensed phase equilibria is relatively small in the low-pressure range, and hence pressure is not considered as a variable in the subsequent discussion on the phase equilibria and thermodynamic properties of condensed phases in these systems.

There are numerous studies reported in literature [1–17] on the determination of phase diagrams of the three Zn–X binaries. The Zn–Te phase diagram is relatively well-known over the whole composition range, while the liquidus in the Zn–Se and Zn–S systems is only known in the Zn-rich regions. However, the melting points of ZnSe and ZnS have been determined. The ZnS phase exists in two allotropic forms; α-ZnS, stable at low temperatures, transforms to β-ZnS at 1020 °C, and β-ZnS melts congruently.

As for the thermodynamic properties of these systems, the Gibbs energies of formation of ZnTe, ZnSe and ZnS have been determined by a number of investigators [18–39]. These data have been assessed by Mills [40]. For the liquid phase, no thermodynamic data are available for the Zn–Se and Zn–S systems whereas for the Zn–Te system

0022-0248/88/$03.50
(North-Holland Physics Publishing Division)

Brebrick [22,23] and Shiozawa et al. [41] have measured the equilibrium partial pressures of Zn(g) and Te_2(g) along the liquidus.

In the present work, the Zn–Te, Zn–Se and Zn–S phase diagrams have been calculated using an associated solution model to describe the thermodynamic properties of the liquid phases and considering ZnTe, ZnSe and ZnS to be line compounds. The model parameters were obtained by simultaneous optimization of the available phase equilibria and thermodynamic data. The calculated phase diagrams agree well with the existing literature data. Agreement between the calculated thermodynamic properties of the liquid phases with the available experimental data is also good.

2. Thermodynamic models

2.1. Liquid phase

An associated solution model is used to describe the thermodynamic properties of the liquid phase. This model has been widely used in the literature to describe the thermodynamic properties of the liquid phase in a number of metal-sulfur, II–VI, IV–VI and III–V systems [42–49]. Schmid and Chang [50] have recently made a review of the associated solution model as applied to metal–nonmetal melts. According to this model, the binary liquid solution of Zn and X (where X stands for Te, Se or S) is considered as a pseudoternary solution of "Zn", "X" and "ZnX" species, governed by an internal equilibrium reaction [50]:

$$\text{“Zn”}(\ell) + \text{“X”}(\ell) = \text{“ZnX”}(\ell), \tag{1}$$

with an equilibrium constant given by:

$$K = \frac{f_3 y_3}{(f_1 y_1)(f_2 y_2)}, \tag{2}$$

where f_1, f_2 and f_3 are the activity coefficients and y_1, y_2 and y_3 are the mole fractions, respectively, of "Zn", "X" and "ZnX" in the liquid phase. The equilibrium constant K may, in general, be expressed as a function of temperature as:

$$\ln K = A/T + B, \tag{3}$$

where A and B are constants. The mole fractions, y_i, are related to the actual mole fractions, x_{Zn} and x_X of Zn and X, respectively, by the following mass balance equations:

$$y_1 = x_{Zn} - x_X y_3, \tag{4}$$

$$y_2 = x_X - x_{Zn} y_3. \tag{5}$$

The excess molar Gibbs energy of the pseudoternary solution is [50,51]:

$$\Delta G^{xs} = RT \times \tfrac{1}{2} \sum_{i=1}^{3} \sum_{j=1}^{3} \left[w_{ij} + (w_{ij} - w_{ji}) y_j - 4 v_{ij} y_i y_j \right] y_i y_j, \tag{6}$$

where w_{ij}, v_{ij}, etc. are the interaction parameters of the solution and $w_{ii} = v_{ii} = 0$ and $v_{ij} = v_{ji}$. The w_{ij} and v_{ij} are, in general, expressed as a function of temperature as:

$$w_{ij} = A_{ij}/T + B_{ij}, \tag{7}$$

$$v_{ij} = C_{ij}/T + D_{ij}, \tag{8}$$

with A_{ij}, B_{ij}, C_{ij} and D_{ij} as constants. The activity coefficients f_i of the species in the pseudoternary solution are then [51]:

$$\ln f_i = \sum_{j=1}^{3} \left[\tfrac{1}{2}(w_{ij} + w_{ji}) + (w_{ij} - w_{ji})\left(\tfrac{1}{2} y_j - y_i\right) - 8 v_{ij} y_i y_j \right] y_j - \sum_{j=1}^{3} \sum_{p=1}^{3} \left[\tfrac{1}{2} w_{jp} + (w_{jp} - w_{pj}) y_p - 6 v_{jp} y_j y_p \right] y_j y_p. \tag{9}$$

The activities of the "Zn" and "X" species are given by:

$$a_1 = f_1 y_1, \tag{10}$$

$$a_2 = f_2 y_2, \tag{11}$$

where a_1 and a_2 are the activities of "Zn" and "X", respectively, with Zn(ℓ) and X(ℓ) as standard states. Since the activities of the "Zn" and "X" species are the same as those of the Zn and X components, respectively [52],

$$a_{Zn} = \gamma_{Zn} x_{Zn} = a_1 = f_1 y_1, \tag{12}$$

$$a_X = \gamma_X x_X = a_2 = f_2 y_2, \tag{13}$$

where γ_{Zn} and γ_X are the activity coefficients of Zn and X in the binary solutions and are different from f_1 and f_2. Once the equilibrium constant K and the interaction parameters w_{ij} and v_{ij} are known, the thermodynamic properties of the liquid solution can be calculated by solving eqs. (2)–(13). The values of these parameters are determined by simultaneous optimization of the phase equilibria and thermodynamic data.

2.2. *ZnX compound phases*

The intermediate phases ZnTe, ZnSe and ZnS are essentially stoichiometric and are therefore considered as line compounds in this study. The Gibbs energy of formation, $\Delta_f G^0$, of the compound ZnX (where X is Te, Se or S) from pure Zn(ℓ) and X(ℓ) is then expressed as a function of temperature as:

$$\Delta_f G^0 = A' + B'T + C'T \ln T, \tag{14}$$

where A', B' and C' are constants.

3. Phase equilibria calculations

3.1. *(L + ZnX) equilibrium*

The liquidus for the compound ZnX may be calculated using the following equation:

$$\bar{G}^L_{Zn} + \bar{G}^L_X = G^0_{ZnX}, \tag{15}$$

where $\bar{G}^L_{Zn}$ and $\bar{G}^L_X$ are the partial molar Gibbs energies of Zn and X, respectively, in the liquid, and G^0_{ZnX} is the Gibbs energy function for the line compound ZnX. Eq. (15) may be rewritten as:

$$^0G^L_{Zn} + RT \ln a^L_{Zn} + {^0G^L_X} + RT \ln a^L_X = G^0_{ZnX},$$

or

$$\begin{aligned} RT\left[\ln a^L_{Zn} + \ln a^L_X\right] &= G^0_{ZnX} - {^0G^L_{Zn}} - {^0G^L_X} \\ &= \Delta_f G^0_{ZnX}, \end{aligned} \tag{16}$$

where a^L_{Zn} and a^L_X are the activities of Zn and X, respectively, in the liquid with respect to pure liquid Zn and X as the standard states, and $\Delta_f G^0_{ZnX}$ is the Gibbs energy of formation for the compound ZnX from pure liquid Zn and X. Eq. (16) can now be solved for the liquidus of ZnX if the activities of Zn and X in the liquid and the Gibbs energy of formation of ZnX are known.

3.2. *(Zn + L) equilibrium*

The mutual solid solubilities of Zn and X (X = Te, Se or S) are essentially zero. Under these circumstances the (Zn + L) equilibrium is given by:

$$^0G^S_{Zn} = \bar{G}^L_{Zn} = {^0G^L_{Zn}} + RT \ln a^L_{Zn},$$

or

$$-RT \ln a^L_{Zn} = {^0G^L_{Zn}} - {^0G^S_{Zn}} = \Delta_{fus}G^0(\text{Zn}), \tag{17}$$

where $\Delta_{fus}G^0(\text{Zn})$ is the Gibbs energy function for the melting of Zn. Eq. (17) may be solved for the liquidus of pure Zn when a^L_{Zn} and $\Delta_{fus}G^0(\text{Zn})$ are known. A similar procedure is used to calculate the liquidus for pure X.

3.3. *($L_1 + L_2$) equilibrium*

Whenever there is a liquid miscibility gap, ($L_1 + L_2$), in the system Zn–X, the equilibrium conditions are given by:

$$\bar{G}^{L_1}_{Zn} = \bar{G}^{L_2}_{Zn}, \tag{18}$$

$$\bar{G}^{L_1}_X = \bar{G}^{L_2}_X. \tag{19}$$

Eqs. (18) and (19) are simultaneously solved for the ($L_1 + L_2$) equilibrium compositions from a knowledge of the thermodynamic properties of the liquid phase.

4. Optimized and/or assessed thermodynamic data

The thermodynamic data for the Gibbs energies of melting of the pure components as well as those for the Gibbs energies of vaporization are taken from the assessed values available in literature [53–55]. The data for the Gibbs energies of formation of the Zn chalcogenide compounds are based on the assessment of Mills [40]. Values of the parameters for the associated solution model

Table 1
Thermodynamic properties of pure components

Function	Expression	Reference
$\Delta_{\text{fus}}G^0(\text{Zn}) = {}^0G^{\text{L}}_{\text{Zn}} - {}^0G^{\text{S}}_{\text{Zn}}$	$7322 - 10.572T$ (J/mol)	Hultgren et al. [53]
$\Delta_{\text{fus}}G^0(\text{Te}) = {}^0G^{\text{L}}_{\text{Te}} - {}^0G^{\text{S}}_{\text{Te}}$	$17489 - 24.20T$ (J/mol)	Hultgren et al. [53]
$\Delta_{\text{fus}}G^0(\text{Se}) = {}^0G^{\text{L}}_{\text{Se}} - {}^0G^{\text{S}}_{\text{Se}}$	$6694.4 - 13.551T$ (J/mol)	Hultgren et al. [53]
${}^0G^{\text{L}}_{\text{S}} - \frac{1}{2}{}^0G^{\text{g}}_{\text{S}_2}$	$-65357 + 165.396T - 13.513T \ln T$ (J/mol)	Sharma and Chang [43], JANAF [54]
$\log p^0_{\text{Zn}}$ (bar)	$-6678.4/T + 9.5787 - 0.55407 \ln T$	Hultgren et al. [53]
$\log p^0_{\text{Te}_2}$ (bar)	$-5960/T + 4.7195$	Hultgren et al. [53]
$\log p^0_{\text{Se}_2}$ (bar)	$-7712/T + 19.346 - 1.7055 \ln T$	Jelinek and Komarek [55]
$\log p^0_{\text{S}_2}$ (bar)	$-6828/T + 17.279 - 1.4117 \ln T$	JANAF [54], Sharma and Chang [43]

are obtained by simultaneous optimization of the available thermodynamic data for the liquid phase, the enthalpies of melting of the ZnX compounds, and the available phase equilibria data. The optimization is carried out using a non-linear regression subroutine. The final optimized/assessed thermodynamic data are summarized in this section.

4.1. Pure components

The enthalpies of melting of pure Zn, Te and Se, assessed by Hultgren et al. [53], are used to obtain the Gibbs energies of melting of these components. The data for the partial pressures of Zn(g), Te_2(g), Se_2(g) and S_2(g) over Zn(ℓ), Te(ℓ), Se(ℓ) and S(ℓ), respectively, are also taken from the literature [53–55]. Table 1 gives the thermodynamic data for the pure components.

4.2. Zn–chalcogenide compounds

The compounds ZnTe, ZnSe and ZnS are essentially stoichiometric and are therefore taken as line compounds in this study. ZnS exists in two allotropic forms [14,40]. The low temperature form α-ZnS, transforms to β-ZnS at 1020°C (1293 K) [14] which is stable to its melting point, 1718°C [6].

The Gibbs energy of formation of ZnTe has been determined by McAteer and Seltze [18] by an EMF method and by Goldfinger and Jeunehomme [19], Pashinkin [20], Lee and Munir [21] and Brebrick [22,23] using dissociation pressure measurements. The enthalpy of formation of ZnTe was measured by Kubaschewski [24] and Pool [25] by calorimetry. Demidenko and Mal'tsev [26] determined the low temperature specific heat of ZnTe. For the ZnSe phase, the Gibbs energy of formation was determined by Woston and Geers [27], Goldfinger and Jeunehomme [19], Pashinkin [20], Sedgwick and Agule [28], Boev et al. [29] and Flogel [30] from dissociation pressure measurements and by Terpilowski and Ratajczak [31] by an EMF method. The Gibbs energy of formation of α-ZnS was determined by Makolkin [32] and Larson and Elliott [33] by an EMF method and by Curlook and Pidgon [34] and Gordeev and Karelin [35] by a gas equilibration method. Goldfinger and Jeunehomme [19], Hirschwald et al. [36] and Munir and Mitchell [37] determined the Gibbs energy of formation of the β-ZnS phase from dissociation pressure measurements. Adami and King [38] measure the enthalpy of formation of β-ZnS by solution calorimetry. The enthalpy of transformation from α-ZnS to β-ZnS at 1293 K was determined by Kapustinsky and Chentzova [39]. All of these data were critically assessed by Mills [40].

In the present investigation, $\Delta_{\text{f}}H^0_{298}$, S^0_{298}, and the $(G^0_T - H^0_{298})/T$ functions of ZnTe, ZnSe and ZnS, assessed by Mills [40], are used along with the $(G^0_T - H^0_{298})/T$ functions for Te from Mills [40], for Zn and Se from Hultgren et al. [53] and for S from the JANAF tables [54], to arrive at the Gibbs energies of formation of these compounds as a function of temperature. The data for the Gibbs energy of formation of each compound

Table 2
Thermodynamic properties of ZnTe, ZnSe and ZnS

ZnTe

$\Delta_f H^0_{298} = -119.2$ kJ/mol, $S^0_{298}(\mathrm{ZnTe}) = 77.8$ J/K·mol
$\mathrm{Zn}(\ell) + \mathrm{Te}(\ell) = \mathrm{ZnTe(s)}$
$\Delta_f G^0 = -147400 + 53.62T$ J/mol; 600–1300 K
$\mathrm{ZnTe(s)} \overset{1573\ K}{\rightleftharpoons} \mathrm{ZnTe}(\ell)$
$\Delta_{\mathrm{fus}} H^0 = 63.9$ kJ/mol

ZnSe

$\Delta_f H^0_{298} = -160.0$ kJ/mol, $S^0_{298}(\mathrm{ZnSe}) = 70.3$ J/K·mol
$\mathrm{Zn}(\ell) + \mathrm{Se}(\ell) = \mathrm{ZnSe(s)}$
$\Delta_f G^0 = -179430 + 45.514T$ J/mol; 600–1300 K
$\mathrm{ZnSe(s)} \overset{1799\ K}{\rightleftharpoons} \mathrm{ZnSe}(\ell)$
$\Delta_{\mathrm{fus}} H^0 = 51.9$ kJ/mol

ZnS

$\Delta_f H^0_{298} = -205$ kJ/mol, $S_{298}(\mathrm{ZnS}) = 57.74$ J/K·mol
$\mathrm{Zn}(\ell) + \frac{1}{2}\mathrm{S_2(g)} = \alpha\text{-}\mathrm{ZnS}$
$\Delta_f G^0 = -274266 + 103.472T$ J/mol; 600–1293 K
$\alpha\text{-}\mathrm{ZnS} \overset{1293\ K}{\rightleftharpoons} \beta\text{-}\mathrm{ZnS}$
$\Delta H^{\mathrm{tr}}_{1293} = 12857$ J/mol
$\mathrm{Zn}(\ell) + \frac{1}{2}\mathrm{S_2(g)} = \beta\text{-}\mathrm{ZnS}$
$\Delta_f G^0 = -261409 + 93.528T$ J/mol
$\beta\text{-}\mathrm{ZnS} \overset{1991\ K}{\rightleftharpoons} \mathrm{ZnS}(\ell)$
$\Delta_{\mathrm{fus}} H^0 = 59.7$ kJ/mol

were then fitted to the equation of the type given by eq. (14) by the least squares method. The results are summarized in table 2.

The enthalpy of melting of ZnTe was determined by Kulwicki [3] from DTA measurements as 64.7 (±5) kJ/mol. Our optimized value is 63.9 kJ/mol which agrees well. The enthalpy of melting of ZnSe has not been experimentally determined. Kubaschewski and Evan [56] estimated it as 52 kJ/mol. For the β-ZnS phase, there is no measured or estimated value for the enthalpy of melting. We have estimated the entropy of melting of β-ZnS phase to be ~ 30 J/K mol, based on the entropy of melting of other II–VI compounds with the same crystal structure. Using this as a starting value, our optimized value for the enthalpy of melting of β-ZnS is 59.7 kJ/mol (ZnS) which yields a value $\Delta_{\mathrm{fus}} S^0 = 34.7$ J/K mol. The assessed/optimized values for the enthalpies of melting for these compounds are also given in table 2.

4.3. Liquid phase

There are no measurements on the thermodynamic properties of the liquid phase in the Zn–Se and Zn–S systems. For the Zn–Te system, Shiozawa et al. [41] and Brebrick [22,23] measured the partial pressures, p_{ZN} and $p_{\mathrm{Te_2}}$, of Zn(g) and $\mathrm{Te_2(g)}$, respectively, along the liquidus, i.e., for the ZnTe + liquid + gas three-phase equilibrium. These data may be converted into the activities of Zn and Te at the liquidus compositions and temperature using the following relations:

$$a_{\mathrm{Zn}} = p_{\mathrm{Zn}}/p^0_{\mathrm{Zn}}, \tag{20}$$

$$a_{\mathrm{Te}} = \left(p_{\mathrm{Te_2}}/p^0_{\mathrm{Te_2}}\right)^{1/2}, \tag{21}$$

where p^0_{Zn} and $p^0_{\mathrm{Te_2}}$ are the equilibrium partial pressures of Zn(g) and $\mathrm{Te_2(g)}$ over pure $\mathrm{Zn}(\ell)$

Table 3
Associated solution model parameters for the liquid phases

Parameter	Zn–Te	Zn–Se	Zn–S
$\ln K$	$-2.0177 + 10638.0/T$	$-2.2293 + 15691.4/T$	$-2.2292 + 20515.3/T$
w_{13}	$0.0 + 3037.5/T$	$0.0 + 1931.0/T$	$-6.5625 + 17151.2/T$
w_{31}	$-5.0132 + 12473.0/T$	$-8.4145 + 18148.5/T$	$w_{31} = w_{13}$
$v_{13} = v_{31}$	$0.0 + 978.0/T$	0.0	0.0
w_{23}	0.0	$-2.2184 + 5679.0/T$	$0.0 - 7399.3/T$
w_{32}	$0.0 + 376.5/T$	$w_{32} = w_{23}$	$0.0 + 6694.6/T$
$v_{23} = v_{32}$	0.0	0.0	0.0
$w_{12} = w_{21}$	0.0	0.0	0.0
$v_{12} = v_{21}$	0.0	0.0	0.0

and Te(ℓ), respectively. The optimum values of the "associated solution model" parameters for these three systems were obtained using the available thermodynamic and phase equilibria data. These parameters are given in table 3.

5. Results and discussion

5.1. Phase diagrams

The calculated Zn–Te, Zn–Se and Zn–S phase diagrams are in good agreement with the experimental data as given in figs. 1 to 6.

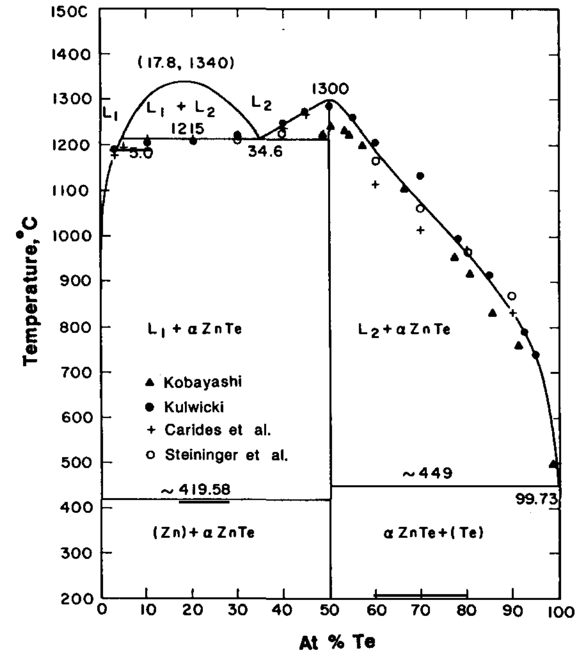

Fig. 1. Comparison between the calculated and experimental Zn–Te phase diagram.

For the Zn–Te system, the melting point of ZnTe was determined as 1239 °C by Kobayashi [1], 1300 °C (±10) by Mason and O'Kane [2], 1290 °C (±10) by Kulwicki [3], 1295 °C (±15) by Carides and Fischer [4] and 1300 °C (±10) by Sysoev et al. [6]. In the present study the melting point of ZnTe is taken to be 1300 °C. The liquidus in the Zn–Te system was determined by Kobayashi [1], Kulwicki [3], Carides and Fischer [4], Reynolds et al. [5] and Steininger et al. [7]. The liquidus data on the Te-rich side have considerable scatter. The calculated liquidus agrees better with the recent determinations by Kulwicki [3], Carides and Fischer [4] and Steininger et al. [7]. On the Zn-rich side, Kulwicki [3], Carides and Fischer [4] and Steininger et al. [7] have concluded, based on their experimental data, that the liquid miscibility gap and the resulting monotectic reaction do not exist. However, after a careful review of their experimental data, we believe a liquid miscibility gap does exist, resulting in the formation of monotectic reaction as given in the calculated phase diagram in fig. 1. Our rationale is given below. According to Carides and Fischer [4], the liquidus temperature increases from 1214 to 1220 °C between 10 and 30 at% Te. This represents only a rise of 6 °C over a concentration range of 20 at% Te; yet their experimental uncertainty is ±20 °C. For the same composition range, Kulwicki [3] obtained an increase in the liquidus temperature from 1208 to 1223 °C, a rise of 15 °C with an experimental uncertainty of ±10 °C. Steininger et al. [7] determined the liquidus temperature at 30 at% Te as 1215.5 °C, which is about the average temperature of the liquidus between 10 and 30 at% Te as determined by Kulwicki [3] and Carides and Fischer [4]. These results, therefore, suggest that within the experimental error the liquidus temperature is virtually constant at ~ 1215 °C between 10 and 30 at% Te. Furthermore, Kulwicki [3] observed double DTA peaks in samples containing 40 and 45 at% Te which they attributed to the inflection in the liquidus and relatively flat liquidus. This explanation is not very convincing. These double DTA peaks can be readily explained by the phase diagram given in fig. 1; one corresponds to the monotectic invariant and the other to the liquidus. However, the extent of the miscibility gap is not known accurately since it is based entirely on the calculation. Fig. 2 shows a comparison between the calculated and experimental data (of Reynolds et al. [5]) for the solubility of ZnTe in liquid Zn at lower temperatures. Reynolds et al. [5] obtained the solubility at these temperatures by dissolving ZnTe crystals in liquid Zn and then determined the solubility either from the weight loss of the crystals (open circles in

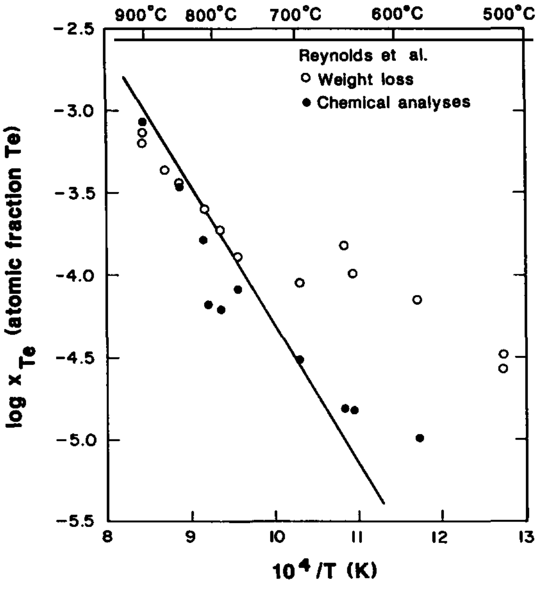

Fig. 2. The solubility of Te in liquid Zn at lower temperatures; comparison between the calculated and experimental data.

fig. 2) or by chemical analysis of the liquid (filled circles in fig. 2). In the present authors' opinion, the data obtained by chemical analysis of the liquid are likely to be more accurate and hence more weight is given to these data. Keeping in mind the experimental difficulties in determining very low solubilities, the agreement between the experimental and calculated low temperature liquidus in fig. 2 is reasonable.

Jordan [46] and Szapiro [48] have also calculated the Zn–Te phase diagram using a regular associated solution model. Both investigators got a reasonable fit with experimental liquidus data for higher Te concentrations; however, they did not use the low temperature liquidus data of Reynolds et al. [5] in the Zn-rich region. Jordan [46] and Szapiro [48] both predicted a liquid miscibility gap and resulting monotectic reaction in the Zn–ZnTe region.

In the Zn–Se system, the melting point of ZnSe was determined to be 1515 °C (±20) by Fischer [8] and 1526 °C (±10) by Sysoev et al. [6]. The liquidus in the Zn–Se system was determined by Ozawa and Hersh [10], Kuzhelev et al. [11], Rubenstein [9] and Kikuma and Furukoshi [12] only up to 9 at% Se. No liquidus data are available for higher Se concentrations. Fig. 3 gives the calculated Zn–Se phase diagram along with the experimental data. The diagram at concentrations higher than about 10 at% Se is entirely based on the calculations, with no experimental phase diagram data input into the optimization process except the melting point of ZnSe. The liquid miscibility gap in the Zn–ZnSe region is predicted by the model. Fig. 4 compares the calculated and experimental liquidus in the Zn-rich region at lower temperatures, and the agreement is very good.

In the Zn–S system, the melting point of ZnS was determined as between 1600 and 1700 °C by Friedrich [13], between 1800 and 1900 °C by Tiede and Schleede [15], 1830 °C (±20) by Addamiano and Dell [16] and 1718 °C (±10) by Sysoev et al. [6]. In the present study, the value of 1718 °C determined by Sysoev et al. [6] is accepted. The Zn–S phase diagram is calculated using the thermodynamic data given in table 1–3 and is given in figs. 5 and 6. As shown in these diagrams the

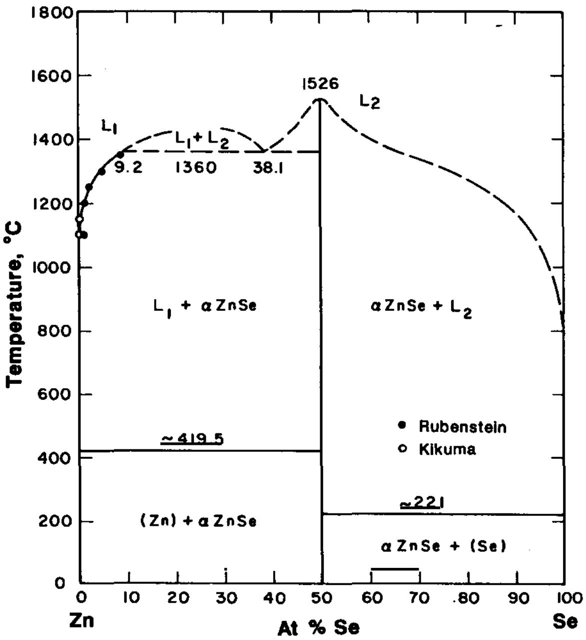

Fig. 3. Comparison between the calculated and experimental Zn–Se phase diagram.

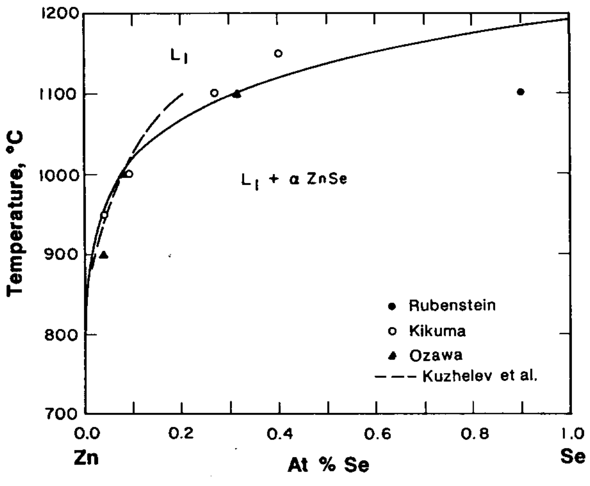

Fig. 4. The Zn-rich region of the Zn–Se phase diagram; comparison between the calculated and experimental data.

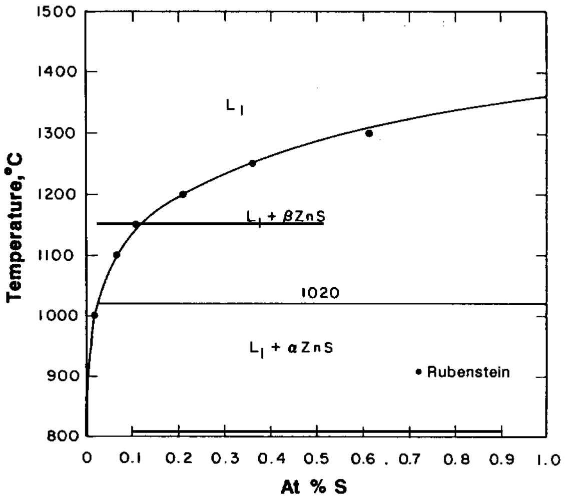

Fig. 6. The Zn-rich region of the Zn–S phase diagram; comparison between the calculated and experimental data.

calculated liquidus at low sulfur concentrations, i.e. < 0.6 at% S is in agreement with the only experimental data, that of Rubenstein [17]. The monotectic temperature for the ZnS–S subsystem is arbitrarily fixed at 1000 °C so that it is lower than the critical point of S, 1040 °C [45]. Since the values of the solution parameters for the liquid phase are derived from the thermodynamic data of ZnS and the liquidus data of Rubenstein [17] at low sulfur concentrations, there are large uncertainties associated with the thermodynamic values of the liquid phase used in the present study. Consequently, the calculated liquid miscibility gaps and the monotectic temperatures are subject to rather large uncertainties.

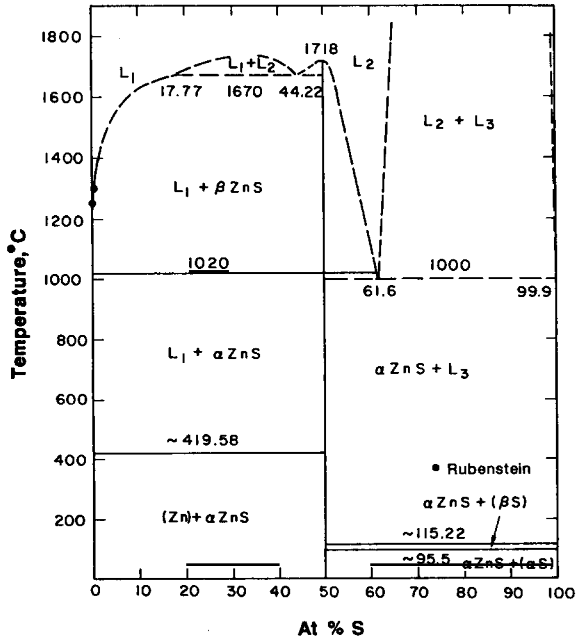

Fig. 5. The calculated Zn–S phase diagram.

5.2. p–T diagrams

Figs. 7 and 8 show the calculated equilibrium partial pressures, p_{Zn} and p_{Te_2}, of Zn(g) and Te_2(g), respectively, along the liquidus in the Zn–Te system. Also shown in these figures are the experimental data of Brebrick [22,33] and Shiozawa et al. [41] and the agreement is, in general, very good. Similar diagrams for the calculated partial pressures p_{Zn} and p_{Se_2} along the liquidus in the Zn–Se system, and p_{Zn} and p_{S_2} along the liquidus in the Zn–S system are given in figs. 9 to 12. No experimental data are available in the Zn–Se and Zn–S systems for comparison.

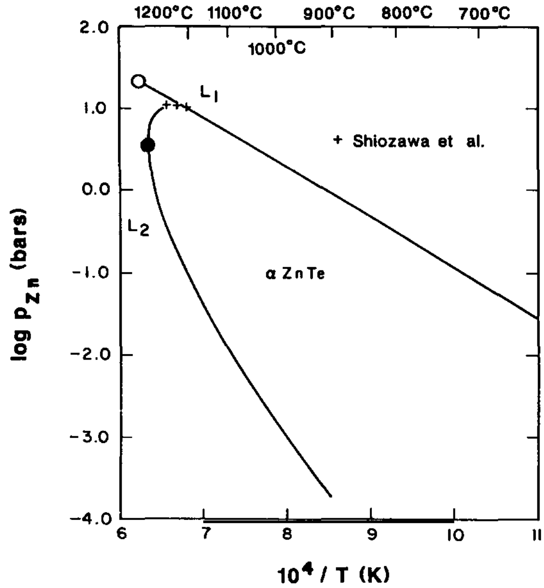

Fig. 7. The equilibrium partial pressure, p_{Zn}, of Zn(g) along the Zn–Te liquidus; comparison between the calculated and experimental data. The solid circle indicates the congruent melting point of α-ZnTe.

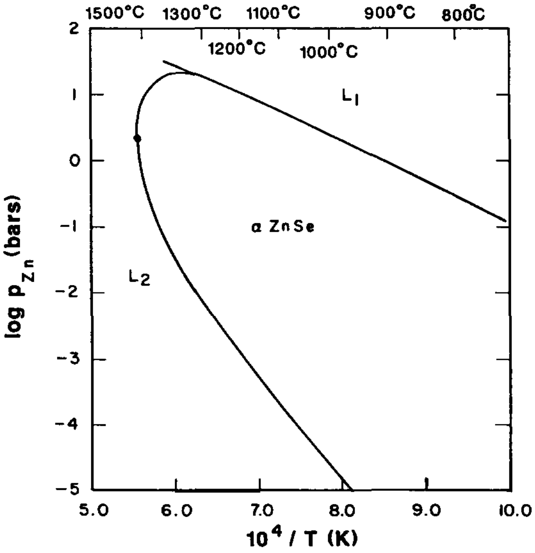

Fig. 9. The calculated equilibrium partial pressure, p_{Zn}, of Zn(g) along the Zn–Se liquidus. The solid circle indicates the congruent melting point of α-ZnSe.

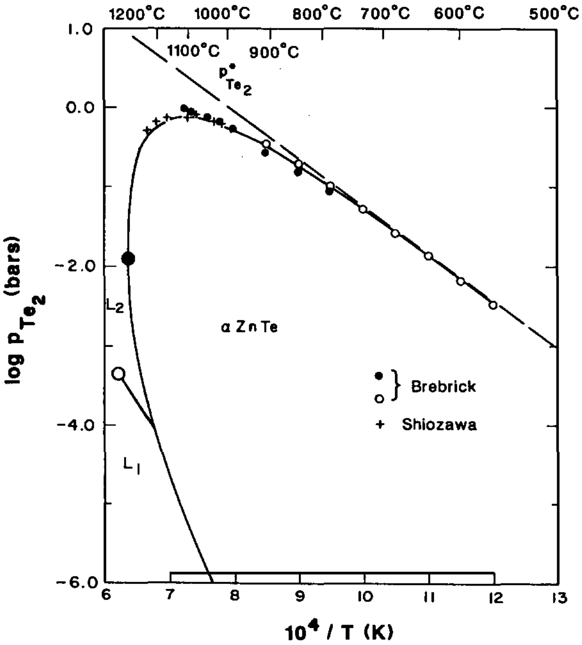

Fig. 8. The equilibrium partial pressure, p_{Te_2}, of Te_2(g) along the Zn–Te liquidus; comparison between the calculated and experimental data. The larger solid circle indicates the congruent melting point of α-ZnTe.

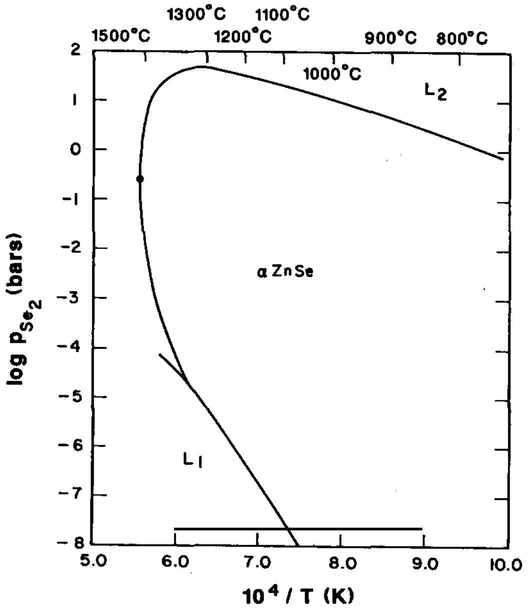

Fig. 10. The calculated equilibrium partial pressure, p_{Se_2}, of Se_2(g) along the Zn–Se liquidus. The solid circle indicates the congruent melting point of α-ZnSe.

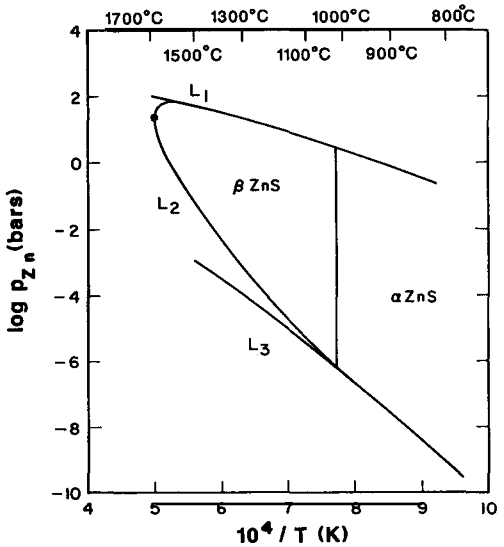

Fig. 11. The calculated equilibrium partial pressure, p_{Zn}, of Zn(g) along the Zn–S liquidus. The solid circle indicates the congruent melting point of β-ZnS.

5.3. Thermodynamic properties of dilute liquid solutions

The thermodynamic properties of dilute solutions are normally expressed in terms of the activity coefficient at infinite dilution and Wagner's self-interaction parameters [57]. Sharma [58] has recently derived the relationships between the associated solution model parameters and the dilute solution parameters. Accordingly, for dilute X (X = Te, Se or S) in liquid Zn, we get:

$$\ln \gamma_X^0 = w_{31} - \ln K, \tag{22}$$

$$\epsilon_X^{(X)} = 2 + 2w_{13} - 4w_{31} - 8v_{13}, \tag{23}$$

$$\rho_X^{(X)} = 2 - w_{13} - w_{31} + 16v_{13}, \qquad (23)$$

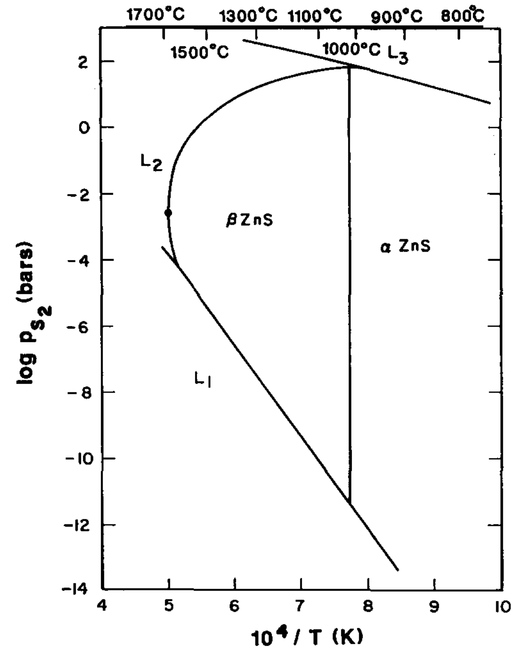

Fig. 12. The calculated equilibrium partial pressure, p_{S_2}, of S_2(g) along the Zn–S liquidus. The solid circle indicates the congruent melting point of β-ZnS.

where γ_X^0 is the activity coefficient of X in liquid Zn at infinite dilution and $\epsilon_X^{(X)}$ and $\rho_X^{(X)}$ are the first and second order Wagner self-interaction parameters, and all other terms are as defined previously.

The activity of X, a_X, in liquid Zn is then given by:

$$\ln a_X = \ln x_X + \ln \gamma_X^0 + \epsilon_X^{(X)} x_X + \rho_X^{(X)} x_X^2. \tag{25}$$

The respective dilute solution parameters for Te, Se and S in liquid Zn obtained from eqs. (22) to (24), are summarized in table 4.

Table 4
Thermodynamic properties of dilute solutions of Te, Se and S in Zn

Parameter	Zn–Te	Zn–Se	Zn–S
$\ln \gamma_X^0$	$-2.9955 + 1835/T$	$-6.1852 + 2457.1/T$	$-4.333 - 3364.1/T$
$\epsilon_X^{(X)}$	$22.0523 - 51641/T$	$35.6580 - 68732.0/T$	$15.125 - 34302.0/T$
$\rho_X^{(X)}$	$7.0132 + 137.5/T$	$10.4145 - 20079.5/T$	$15.125 - 34302.0/T$

6. General discussion

In the foregoing calculations, the optimum values of the associated solution model parameters for the liquid phases are arrived at by simultaneous optimization with respect to all the available phase diagrams as well as thermodynamic data. A minimum number of parameters, that adequately describe the experimental data are used. These parameters are quite sensitive to the phase equilibria as well as thermodynamic data. Since, in these systems, the thermodynamic information for the liquid phases is very limited or non-existence, in addition to phase diagram data, the minimum thermodynamic information required to obtain a optimal set of parameters for the liquid phases are the Gibbs energies for the formation and melting of the intermediate compounds.

Acknowledgement

The authors wish to thank Ken Vlach for review of the manuscript.

References

[1] M. Kobayashi, Intern. Z. Metallogr. 2 (1912) 65.
[2] D.R. Mason and D.F. O'Kane, Preparation and Properties of Some Semiconducting Compounds (Academic Press, New York, 1961).
[3] B.M. Kulwicki, PhD Thesis, The University of Michigan, Ann Arbor, MI (1963).
[4] J. Carides and A.G. Fischer, Solid State Commun. 2 (1964) 217.
[5] R.A. Reynolds, D.G. Stroud and D.A. Stevenson, J. Electrochem. Soc. 114 (1967) 1281.
[6] L.A. Sysoev, E.K. Raiskin and V.R. Gur'ev, Inorg. Mater. 3 (1967) 341.
[7] J. Steininger, A.J. Strauss and R.F. Brebrick, J. Appl. Phys. 117 (1970) 1305.
[8] A.G. Fischer, J. Electrochem. Soc. 106 (1959) 838.
[9] M. Rubenstein, J. Crystal Growth 3/4 (1968) 309.
[10] L. Ozawa and H.N. Hersh, J. Electrochem. Soc. 230 (1973) 938.
[11] L.P. Kuzhelev, I.A. Mironov, V.N. Pavlova and I.M. Stroganova, Russ. J. Phys. Chem. 48 (1974) 287.
[12] I. Kikuma and M. Furukoshi, J. Crystal Growth 50 (1980) 654.
[13] K. Friedrich, Metallurgie 5 (1908) 114.
[14] E.T. Allen and J.L. Crenshaw, Am. J. Sci. 34 (1912) 341.
[15] E. Tiede and A. Schleede, Ber. Deut. Chem. Ges. 53B (1920) 1717.
[16] A. Addamiano and P.A. Dell, J. Phys. Chem. 61 (1957) 1020.
[17] M. Rubenstein, J. Crystal Growth 41 (1977) 311.
[18] J.H. McAteer and H. Seltze, J. Am. Chem. Soc. 58 (1936) 2081.
[19] P. Goldfinger and M. Jeunehomme, Trans. Faraday Soc. 59 (1964) 2851.
[20] A.S. Pashinkin, Russ. J. Phys. Chem. 38 (1964) 1461.
[21] W.T. Lee and Z.A. Munir, J. Electrochem. Soc. 114 (1967) 1236.
[22] R.F. Brebrick, J. Electrochem. Soc. 116 (1969) 1274.
[23] R.F. Brebrick, J. Electrochem. Soc. 118 (1971) 2014.
[24] O. Kubaschewski, Z. Elektrochem. 47 (1941) 623.
[25] M.J. Pool, Trans. TMS-AIME 233 (1965) 1711.
[26] A.F. Demidenko and A.K. Mal'tsev, Inorg. Mater. 5 (1969) 130.
[27] W.J. Woston and M.G. Geers, J. Phys. Chem. 66 (1962) 1252.
[28] T.O. Sedgwick and B.J. Agule, J. Electrochem. Soc. 113 (1966) 54.
[29] E.I. Boev, L.A. Bendeski and G.A. Milkov, Russ. J. Phys. Chem. 43 (1969) 776.
[30] P. Flogel, Z. Anorg. Chem. 370 (1969) 16.
[31] J. Terpilowski and E. Ratajczak, Roczn. Chem. 41 (1967) 429.
[32] I.A. Makolkin, Acta Phys. URSS 13 (1940) 361.
[33] H.R. Larson and J.F. Elliott, Trans. TMS-AIME 29 (1967) 1713.
[34] W. Curlook and L.M. Pidgeon, Trans. TMS-AIME 212 (1958) 671.
[35] I.V. Gordeev and V.V. Karelin, Inorg. Mater. 5 (1969) 1012.
[36] W. Hirschwald, G. Neumann and I.N. Stranski, Z. Physik. Chem. 45 (1965) 170.
[37] Z.A. Munir and M.T. Mitchell, High Temp. Sci. 1 (1969) 381.
[38] L.H. Adami and E.G. King, US Bur. Mines, Rept. Investn. 6495 (1964).
[39] A.F. Kapustinsky and L.G. Chentzova, Compt. Rend. Acad. Sci. URSS 30 (1941) 489.
[40] K.C. Mills, Thermodynamic Data for Inorganic Sulphides, Selenides and Tellurides (Butterworths, London, 1974).
[41] L.R. Shiozawa, J.M. Jost and G.A. Sullivan, Research on Improved II–VI Compounds, Final Report, Contract AF 33 (615)–2708, Aerospace Research Labs, USAF, Wright-Patterson Air Force Base, Ohio (1965–68). Quoted by Jordan [42].
[42] A.S. Jordan and R.R. Zupp, J. Electrochem. Soc. 116 (1969) 1264.
[43] R.C. Sharma and Y.A. Chang, Met. Trans. B, 10B (1979) 103.
[44] R.C. Sharma and Y.A. Chang. Met. Trans. B, 11B (1980) 139.

[45] Y.-Y. Chuang, K.-C. Hsieh and Y.A. Chang, Met. Trans. B, 16B (1985) 277.
[46] A.S. Jordan, Met. Trans. 1 (1970) 239.
[47] T. Tung, L. Golonka and R.F. Brebrick, J. Electrochem. Soc. 128 (1981) 1601.
[48] S. Szapiro, J. Electron. Mater. 5 (1976) 223.
[49] R.F. Brebrick, C.H. Su and P.K. Liao, in: Semiconductors and Semimetals, Vol. 19, Eds. R.K. Willardson and A.C. Beer (Academic Press, New York, 1983) pp. 171–253.
[50] R. Schmid and Y.A. Chang, CALPHAD 9 (1985) 363.
[51] Y.-Y. Chang, R. Schmid and Y.A. Chang, Met. Trans. A, 15A (1984) 1921.
[52] I. Prigogine and R. Defay, Chemical Thermodynamics (Longmans, Green and Co., London, 1965) pp. 410–411
[53] R. Hultgren, P.D. Desai, D.T. Hawkins, M. Gleiser, K.K. Kelley and D.D. Wagman, Selected Values of the Thermodynamic Properties of the Elements (Am. Soc. for Metals, Metals Park, Ohio, 1973).
[54] JANAF Thermochemical Tables, 2nd ed. (National Bureau of Standards, Washington, DC, 1971).
[55] H. Jelinek and K.L. Komarek, Monatsh. Chem. 105 (1974) 689.
[56] O. Kubaschewski and E.L. Evans, Metallurgical Thermochemistry (Wiley, New York, 1956) p. 189.
[57] C. Wagner, Thermodynamics of Alloys (Addison-Wesley, Reading, MA, 1952) pp. 47–53.
[58] R.C. Sharma, Met. Trans. A, 18A (1987) 1641.